International Journal of Nanoscience
Vol. 20, No. 3 (2021) 2150022 (11 pages)
© World Scientific Publishing Company
DOI: 10.1142/S0219581X21500228

World Scientific
www.worldscientific.com

Lidocaine Hydrochloride Nanoparticles Preparation using Multiple Emulsions and its Physicochemical Evaluation

Nader Shakiba-Maram[*,¶], Omid Kheiry Avarvand[†,‖], Neda Mohtasham[‡,**] and Amanollah Zarei Ahmady[§,††]

[*]*Nanotechnology Research Center*
Ahvaz Jundishapur University of Medical Sciences
Ahvaz, Iran

[†]*Student Research Committee*
Ahvaz Jundishapur University of Medical Sciences, Ahvaz, Iran

[‡]*Department of Pediatric Clinical Toxicology*
Abuzar Children's Medical Center
Ahvaz Jundishapur University of Medical Sciences
Ahvaz, Iran

[§]*Marine Pharmaceutical Science Research Center*
Ahvaz JundiShapur University of Medical Sciences
Ahvaz, Iran

[¶]*shakiba1967@gmail.com*
[‖]*omidkheiry@hotmail.com*
[**]*mohtasham-n@ajums.ac.ir*
[††]*zarei-a@ajums.ac.ir*

Received 31 October 2020
Accepted 25 January 2021
Published 8 May 2021

Lidocaine is a primary local anesthesia that blocks the ionic fluxes required for the beginning and operation of impulses in the neuronal membrane. The benefits of local anesthetics, such as enhancing patient acceptance, prohibiting systemic toxicity and delivering continuous drug delivery, make them the attracting field for pharmaceutical researchers. The nanoparticles were prepared by solvent evaporation $W_1/O/W_2$ emulsion method and in the ratios of 1 to 1, 1 to 2 and 1 to 3 drug to polymer. The production yield, loading efficiency, particle size, poly dispersity index and zeta potential of selected formulation were 84.30%, 80.60%, 192 nm, 0.18 mV and +42.8 mV, respectively. DSC and FTIR studies showed that no chemical interactions between drug and polymer Formulations showed an initial burst release, which is a reason for the good capacity of the polymer to maintain the drug in it and lead to a primary slow release.

Keywords: Lidocaine hydrochloride; nanoparticles; drug delivery; multiple emulsion; novel drug delivery; nanotechnology.

[††] Corresponding author.

1. Introduction

Lidocaine, as a first modern local anesthetic agent, was synthesized and formulated in 1940 and 1943, respectively.[1] Its IUPAC name is 2-(diethyl amino)-N-(2,6-dimethyl phenyl) acetamide and is used topically to reduce itching, burning and pain from skin infection. Lidocaine strengthens the neuronal membrane by blocking the ionic fluxes required for the beginning and operation of impulses, thereby effecting local anesthetic action. Local anesthetics work through the repeatable inhibition of action potential production and development with the pharmacological properties figured out by their molecular structure which consists of an aromatic ring referring lipophilicity and potency, an intermediate chain as specification of stability and an amine group (Fig. 1).[2]

Due to these properties, most local anesthetics need a needle to bypass the skin barrier and cater effective dermal anesthesia. Local anesthetics of the amide type are thought to accomplish within the sodium channels of the nerve membrane. Lidocaine is an effective and dependable local anesthetic of rapid beginning, intermediate action, and low systemic toxicity. The marketed preparation of Lidocaine includes topical ointment, gel and solution which contains Lidocaine hydrochloride in different concentrations limiting from 1–5% w/w; Lidocaine ointment 5% is formulated for temporary reduction of pain associated with minor burns and abrasions of skin, e.g., sunburns, herpes zoster, insect bites, hemorrhoids and fissures. Lidocaine is inefficient when applied to nonwounded skin. Lidocaine is often used to relief pain after surgery, trauma, or medical procedures.[3]

Permeation of local anesthetics into the wound decreases post-operative pain and provides to a more rapid improvement and mobilization. It would be exclusively useful if durable local anesthesia could be supplied by loading local anesthetics into delivery systems. The skin, the largest organ of the body, may be considered either as a natural protective barrier against penetration of toxic foreign substances, excessive loss of water and other fundamental compounds, or as a guaranteed gate of entry of drugs for local and/or systemic action. In percutaneous applications, the drug should stay on the skin surface as potential function in lipophilic form for a considerable time, so that it penetrates the stratum corneum and anaesthetizes the principal pain receptors within the skin.[2]

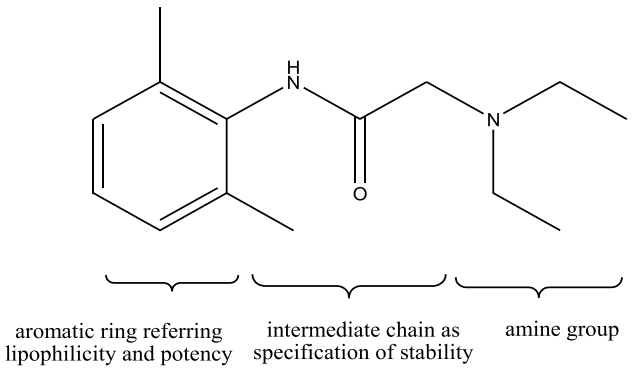

Fig. 1. Components of the lidocaine structure.

Drug delivery of anesthetics to the skin presents both unique chance and obstructions due to skin structure, physiology and barrier properties. Inadequate permeability due to skin barrier, such as the stratum corneum, is one of the most important obstructions which limits their clinical application, compared to the injection. The benefits for local anesthetics, such as enhancing patient acceptance, prohibiting systemic toxicity and delivering continuous drug delivery, make them the attracting field for pharmaceutical researchers. Their action is defined by a rapid but short effect, in comparison with the potential duration of pain.[4] Thus, it is necessary to advance effective and prolonged local transdermal anesthetics. Transcutaneous delivery proffers an alternative to injecting the local anesthetics. The drug, however, has to be in a solubilized form, to allow passive diffusion via the skin, which is controlled by a concentration gradient. The original crystalline anesthetic drugs are solubilized to permit their entry within the formulation in high concentration and thus, increasing their permeation through the skin.[5]

Modern topical drug delivery systems, such as bit carriers, are now being designed to make a drug capable of arriving at the functional Pharmacological site at a controlled rate and have a sustained time of action. Targeting of topically exerted drugs to the skin layers by using bit carriers has become a main center of research in dermatology. A number of carrier systems like micro emulsion, liposomes and nanoparticles have been explored for percutaneous delivery of drugs. These systems may improve drug permeation in skin, increase time of local action and prevent systemic absorption of drugs and consequently decrease side effects relevant to the drugs.[4]

Optimization of local anesthesia utilizations for higher permeation and bioavailability comprises of

interactions between the formulation and the molecular components of the skin barrier. Nowadays, the expansion of local anesthetics skin-delivery systems using liposomes or lipid nanoparticles has been searched as substitutes to commercial formulations such as Lidocaine and Prilocaine cream. Adjusting the release rate of drugs causes improving bioadhesive properties reducing toxicity and ensuing to an improved therapeutic efficiency.[6,7]

Nanoemulsions (NEs) are thermodynamically stable systems consisting of a hydrophilic and a hydrophobic phase, permanent with the use of surfactants. Stable NEs consist of nanometer-sized hydrocarbon domains encircled by amphiphilic molecules, reliable in a continuous aqueous phase. Nanoparticles are a type of colloidal drug delivery system that consists of particles with a diameter of 10 to 1000 nanometers. Nanoparticles may exhibit properties that differ significantly from those observed in coarse particles W/O NEs are special attention because a type of reactants can be presented into the nanometer-sized aqueous domains for reaction restricted within the reverse micelles, resulting in materials with controlled size and shape.[8]

The main benefits of nanoparticles are the improvement of bioavailability with increasing the solubility in water and increasing the resistance time in the body (increasing the half-life). Placing the drug in a specific site in the body (site of its effect) is safe for toxic therapies and protects non-target tissues and cells from severe side effects. The nanoparticle is coated with a polymer that releases the drug across the membrane or matrix of the polymer by controlled diffusion or erosion. Membrane coating acts as a barrier to release, therefore, the solubility and penetration of the drug into the polymer membrane become the determining factor in drug release. In addition, the rate of release can be affected by ionic interactions between the drug and other substances. When the drug interacts with the excipients to form a water-soluble complex, the drug release can be very slow and has almost without the burst release.[9]

In special circumstances, by encapsulating the therapeutic drug, leading to nanoscale range particles, which is smaller than the basic crystalline drug size while being capable of enhancing the aqueous solubility of the anesthetics multifold. Their increased surface area-to-volume ratio leads to increased permeation via all routes through the skin containing intracellular, intercellular and trans-appendageal route. There are many different classes of nanocarriers related to the material used in the provisions. If drugs are formulated as nanoparticles, penetration into the infective tissue is appropriate and their effect is increased.[5]

In this study, due to the slow elimination of nanoparticles in the body and their greater effect compared to ordinary particles and due to the high consumption of lidocaine, lidocaine as a nanoparticle was formulated to increase the effect and duration of anesthesia and the decreased amount of usage.

2. Materials and Methods

2.1. *Source of used materials*

All chemicals and solvents were purchased from Sigma Aldrich (Dorset, UK). The artificial skin (cellulose acetate membranes, Visking dialysis tubing, cut-off: 10 KDa, diameter: 2 cm) was bought from Medicell Membranes Ltd (London, UK). The laboratory equipment received were made by Soham Scientific Ltd (Fordham, UK).

2.2. *Preparation of Lidocaine nanoparticles*

With respect to Lidocaine hydrochloride solubility in water, the nanoparticles were prepared by solvent evaporation $W_1/O/W_2$ emulsion method. In the first step, an initial emulsion W_1/O was formed, where 100 mg of the drug was dissolved in 5 mL of water as the internal aqueous phase. Then this phase was taken in 20 mL of methylene chloride containing 100 mg, 200 mg and 300 mg of Eudragit RS-100 polymer under the homogenizer at 24 000 RPM. The content was then added to 25 mL of 0.2% polyvinyl alcohol solution and nanoparticles container was placed under a 1000 rpm agitator for 2 h to remove the solvent. Centrifuged nanoparticles (18 000 g) were dispersed in 5 mL of water and were lyophilized. Three samples were prepared from each formulation.

2.3. *Characterization of Lidocaine nanoparticles*

2.3.1. *Particle size measurements*

All formulations were diluted with de-ionized water (1 to 200 V/V) prior to particle size measurements,

which were carried out using photon correlation spectroscopy (Malvern Zetasizer Nano-ZS, Malvern Instruments, Worcestershire, UK). The accuracy of the instrument was achieved intermittently using a drop of latex beads (polystyrene, mean size: 0.1 μm, Sigma) in 50 mmol sodium chloride. All measurements ($n = 9$) were accomplished in triplicate and the mean particle size and standard deviation of the formulations was calculated. The polydispersity index (PDI) was obtained from the following equation[10]:

$$\mathrm{PDI} = \frac{\mathrm{SD}^2}{\mathrm{mean}^2}. \quad (1)$$

2.3.2. *Production yield*

After the lyophilization of the nanoparticles, the production yield was calculated by the following equilibrium[11]:

$$\text{Production yield} = \frac{\text{Weight of freeze dried nanoparticles (mg)}}{\text{Weight of drug (mg)} + \text{Polymer (mg)}} \times 100. \quad (2)$$

2.3.3. *Loading efficiency*

Nanoparticles suspension was centrifuged (18 000 g) for 20 min at 25°C. 10 mL of the supernatant containing unloaded Lidocaine was inserted into the dialysis bag. The dialysis bag was put into a Becher containing 20 mL of PVA (0.2%). The Becher was stirred on a magnetic stirrer for 1 h (50 RPM) at room temperature to let the solutions become equilibrated with each other. Afterwards, the Becher was let at room temperature for 5 days to decrease the solution volume to 5 mL, so that its UV absorption could be detected by spectrophotometer (Cecil England, CE2501). Finally, the unloaded drug absorption was measured by UV spectrophotometry at 264 nm. Entrapment efficiency (EE%) was calculated using the calibration curve and the following equilibrium[12]:

$$\mathrm{EE}\% = \frac{\text{Amount of drug in the formulation (mg)} - \text{amount of unloaded drug in supernatant (mg)}}{\text{Amount of drug in the formulation(mg)}} \times 100. \quad (3)$$

2.3.4. *Transmission electron microscopy (TEM) imaging*

A drop of the solution was placed on Formvar/Carbon Coated Grid Excess sample was filtered off and negatively stained with 2% cleanly prepared aqueous uranyl acetate. Imaging was performed under a Jeol JEM 1400 TEM (Hertfordshire, UK). The Digital images were taken by an AMTV600 digital camera.

2.3.5. *FTIR spectroscopy*

The Fourier Transform Infrared Spectroscopy (FTIR) spectroscopy gives a lot of information about the composition of the compounds. Only certain frequencies of infrared radiation are absorbed by the molecule and cause tensile and flexural vibrations of covalent bonds. The energy absorbed by specific functional groups at a certain wavelength will reduce the intensity of light transmission and is usually plotted as a function of the wave number. The infrared spectrum can be used to identify molecules, like fingerprints in humans. The simplest form of vibrational movements, bending and tensile movements is the flexing movement which is easier than tensile movement. The scan range was 450–4000 cm^{-1} and the scan accuracy was 4 cm^{-1}. Processing of the FTIR results was performed with GRAMS/32 Version 3.04 software.

2.3.6. *DSC studies of Lidocaine nanoparticles*

Without Lidocaine and Lidocaine-loaded nanoparticles were freeze dried. The thermograms of particular components and nanoparticles were recorded on Chromatopac R6A (Shimadzu, Japan) thermal analyzer. An accurately weighed amount (5 mg) of individual components was transferred to aluminum pans and the samples (nanoparticles, Lidocaine and Eudragit RS-100) were scanned from 20°C to 200°C at the heating rate of 10°C/min using an empty aluminum pan as reference.

2.3.7. *XRD studies of Lidocaine nanoparticles*

X-ray diffraction patterns (XRD) were took down to assess the physical nature of the formulations. Without Lidocaine and Lidocaine-loaded nanoparticles were freeze dried so as to keep the formulation in powdered form. XRD patterns were recorded on a powder X-ray diffractometer at a

scanning rate of $2^\circ\,min^{-1}$ between 10° and 60° 2θ range.[13]

2.3.8. *Zeta potential studies of Lidocaine nanoparticles*

The zeta potential of the nanoparticles was taken by the measuring of the electrophoretic mobility using a 90 plus particle size analyzer. The conversion of the electrophoretic mobility to zeta potential was accomplished using the following Helmoltz–Smoluchowski equation:

$$\zeta = E(4\pi\eta/\varepsilon), \tag{4}$$

where ζ is the zeta potential (mV), E is the electrophoresis mobility, η is the viscosity of the dispersion medium (water 0.8904 cp) and ε is the dielectric constant of the solvent (water, 78.54).

Whilst, it is well known about the Helmoltz–Smoluchowski equation (4). Before that, the electrophoretic mobility measurements and all the samples were diluted with ultra-purified water and the measurements were performed at 25°C.[14]

2.4. *Stability studies of Lidocaine nanoparticles*

The optimized nanoparticles and nanoparticles dispersions were investigated for stability. The formulations were stored at $4 \pm 2^\circ$C, $25 \pm 2^\circ$C, $40 \pm 2^\circ$C and relative humidity (RH) $75 \pm 5\%$ for a period of 6 months and aliquots were removed for analyzing at periods of 0, 15, 30, 60, 90 and 180 days. The formulations were assessed with regard to maintained Lidocaine percent, particle size and PDI.[15]

2.5. *In vitro diffusion studies*

In vitro static diffusion cells are accredited and widely used method to assess skin permeability of developed formulations. Artificial membranes in connection with diffusion studies are used on human skin models. After the chambers were filled up with 2 mL of acetate buffer, washed cellulose acetate membranes (10 kDa) were cut into square pieces and picked up to adequately cover the receptor chambers. The formulations (1 mL or 1 g) were placed in the donor compartment, which were sealed with the stirrer (350 rpm). Samples were removed at 0, 1, 2, 4 and 6 h from the receiver compartment, and an equal volume of pre-heated acetate buffer was replaced.

2.5.1. *Dissolution studies*

The *in vitro* release profile of Lidocaine from the polymeric nanoparticles was studied by the dialysis bag diffusion technique and under sink condition for all three formulations. The dialysis bag retained nanoparticles and allowed the diffusion of the free drug immediately into the recipient compartment. 80 mg of the lyophilized nanoparticles was added to 10 mL of phosphate buffer (pH = 7.4) stimulating the intestinal medium in the dialysis bag and put into 20 mL of dissolution medium in a Becher on the magnetic stirrer, maintained at $37 \pm 1^\circ$C and then, stirred at 50 rpm. Samples from the Becher 0.5, 1, 2, 4, 6, 8, 12 and 24 h intervals were analyzed. The UV absorption of the solutions was measured at 264 nm.

2.5.2. *Dissolution kinetic*

The *in vitro* release profiles were fitted to various kinetic models (Higuchi, First-order, Zero-order, Peppas, Hixson-Crowell, Square root of mass, Three second root of mass, Weibull, linear probability and log-probability) in order to determine the drug release mechanism.[16] Slope of the respective plots was used to calculate the rate constants. The obtained data were also put in the Korsemeyer–Peppas model in order to find out n value, which indicates the drug release mechanism.

2.5.3. *Lidocaine concentration in the receiver fluid data analysis and statistical analysis*

All data calculate standard deviations and fit linear equations. One-way analysis of variance (ANOVA) with *post hoc* Tukey test was used to evaluate differences in permeation across cellulose membranes, where $p < 0.05$ was regarded statistically significant using Minitab 16. The results were remarked as mean ± standard deviation. Statistical analysis was carried out on the data sets with analysis of variance differences were regarded significant for $p < 0.05$.

3. Results and Discussion

Many methods have previously been recounted for the preparation of nanoparticles such as high sheer homogenization, high pressure homogenization, solvent diffusion, emulsification and solvent evaporation methods.[17] A simple nanoemulsion-based

method, with organic solvents and satisfactory for up-scale reduction, was used in this study.

3.1. *Production yield*

The production yield of the formulations is shown in Table 1. The production yield of F_c (92.20%) was not significantly more than F_a (76.71%) with the (p value > 0.05) and with F_b (84.30%) with the (p value of 0.34), also there is no significant difference between F_b and F_a (p value of 0.32). Since the total amounts of the drug and polymer in F_c are more than F_a and F_b, the ratio of the waste substances to the production material was less than F_a and F_b, therefore, the ratio of the nanoparticles dry mass to the row material was used and the production yield was smaller in F_a.

3.2. *Loading efficiency*

Loading efficiency for F_c, F_b and F_a was calculated as 88.90%, 80.60% and 71.35%, respectively, (Table 1). There didn't exist any significant difference between the loading efficiencies of F_c and F_b and also between the F_b and F_a (p value > 0.05). Loading efficiency between F_c and F_a has significant difference (p value $= 0.05$). Larger percentage of F_c loading efficiency compared to F_a and F_b was due to the bigger amount of polymer, which was also observed in the research of Nath *et al.*[18] Generally, the loading efficiencies of the formulations were acceptable. Probably, by increasing the polymer-to-drug ratio, more drug particles are trapped inside the nanoparticles. By changing the speed of the homogenizer, there was no significant change in the loading efficiency.

3.3. *Particle size and polydispersity*

The mean particle size and PDI of all formulations is demonstrated in Table 1. Obtained mean particle size for F_a, F_b and F_c was 170 nm, 192 nm and 215 nm, respectively. There didn't exist any significant difference between the particle size of F_a and F_b and also between the F_b and F_c (p value $= 0.20$ and 0.23, respectively), but there was a significant difference between the particle sizes of the F_a, and F_c formulations (p value < 0.05). Adibkia *et al.* also reported the similar particle size of nanoparticles with Eudragit RS-100: drug ratio of 1:1 and 3:1.[19]

The mean particle size in F_c was a little bigger than F_a and F_b for the reason of higher amount of polymer in the formulation that leads to the thicker organic solution, larger emulsion droplets and particle size, which was observed in Nath *et al.*'s research on Zidovudine microspheres, as well.[18]

The PDI, as shown in Table 1 for all three formulations, was less than 0.3, which is considered to be acceptable for polymer-based nanoparticles.[20] The difference between the PDI of the formulations was not significant (p value > 0.05). The uniform distribution of the nanoparticles size is helpful, since it leads to predictable pharmacokinetics.

3.4. *Zeta potential*

The zeta potential of F_c, F_b, F_a, pure drug and pure polymer was measured as +44.9, +42.8, +40.9, +3.17 and +55.1, respectively. As Eudragit RS-100 surface charge is positive, the encapsulation of the drug into the polymer was confirmed and as demonstrated by Scanning Electron Microscopy (SEM) imaging, it has made a uniform polymeric coating. The surface charge of the nanoparticles influences their distribution and absorption into the cells. Because of the negative charge of the cell membrane, there is most electrostatic desire to the positively charged particles. In addition, the suspended particles may be absorbed faster than the coagulated ones. The measured zeta potential is sufficient for providing a good stability and inhibits the aggregation of the nanoparticles.[21]

3.5. *Scanning electron microscopy*

The SEM images demonstrated that the nanoparticles had a spherical and relatively uniform

Table 1. The mean production yield, mean loading efficiency, mean particle size, mean PDI and mean zeta potential of F_a, F_b and F_c.

Formulation	Mean production yield ± SD (%)	Mean loading efficiency ± SD (%)	Mean particle size ± SD (nm)	Mean PDI ± SD	Mean zeta potential (mV)
F_a	76.71 ± 7.15	71.35 ± 7.25	170 ± 15.3	0.15 ± 0.013	+40.9
F_b	84.3 ± 8.25	80.6 ± 7.68	192 ± 18.35	0.18 ± 0.017	+42.8
F_c	92.2 ± 8.53	88.9 ± 8.24	215 ± 20.57	0.19 ± 0.022	+44.9

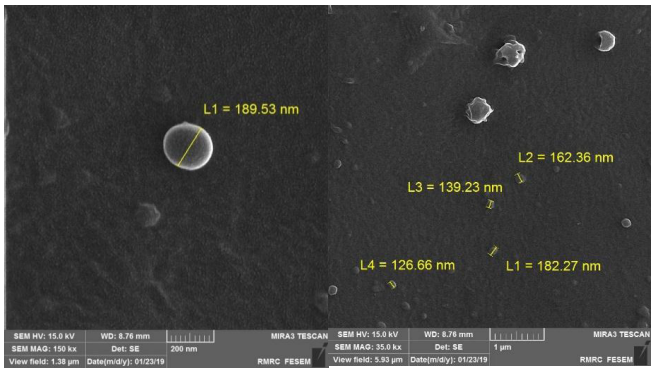

Fig. 2. SEM images of F_b formulation.

surface (Fig. 2). According to the spherical shape of the nanoparticles, pharmacokinetic through the body would be somehow more predictable.

3.6. *Differential scanning calorimetry (DSC)*

The results of DSC analysis are shown in Fig. 3. The large and sharp peak at 80°C was observed in the thermograms of drug and formulations. The presence of the polymer in the formulations made this peak wider in comparison with the pure drug and the higher ratio of polymer in F_c led to a wider peak than F_a. Less amount of the drug in F_a sample compared to F_c caused the peak height to be shorter. In the case of the nanoparticles, the mentioned peak was shorter than the pure drug, as well. The reduction in intensity of the peak related to the drug was assumed to be related to the solubilization of the drug in the polymeric matrix or the heating induced solid state interactions.[22]

Based on DSC technique, interactions between the drug and the polymer revealed that Eudragit RS-100 stabilized Lidocaine in the nanoparticles structure and the enhancement in the polymer amount increases its stability. On the other hand, by changing the polymer: drug ratio, it was evolved that physical interactions between the polymer and the drug contributed in thermal stability of Eudragit RS-100 to a large extent. Physical nature of these interactions was concluded by FTIR

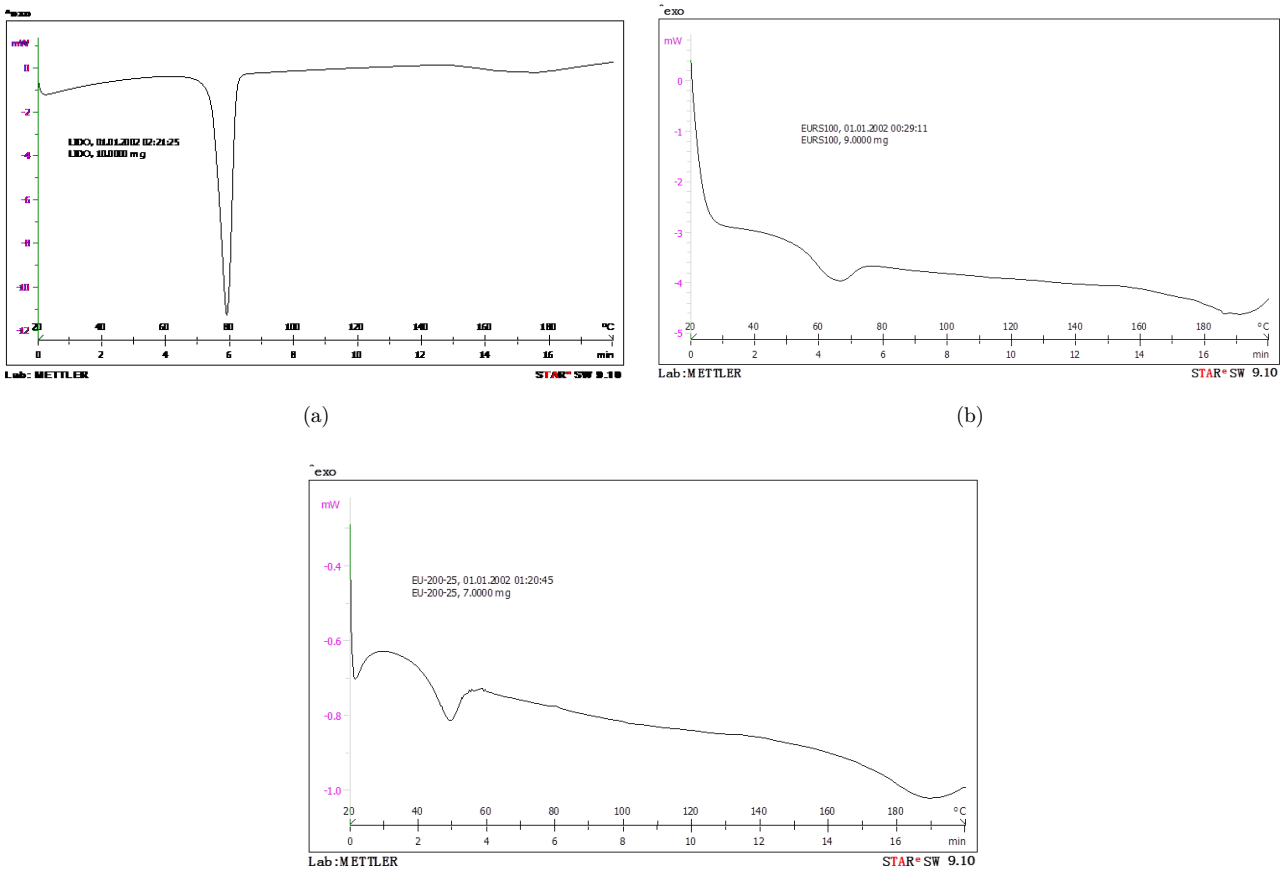

(a) (b)

(c)

Fig. 3. DSC thermogram of (a) Lidocaine hydrochloride, (b) Eudragit RS-100 and (c) F_b formulation.

spectra of the nanoparticles. The presence of the drug peak in the formulations demonstrated the maintenance of Lidocaine crystallinity in the nanoparticles. Almost all the changes in the drug peaks exist in the formulations thermograms, demonstrating the presence of the drug in all formulations. The percentage of the drug thermal decomposition reduced in all the formulations. This indicates the thermal stability of the drug in the presence of the polymer, causing the stability of the prepared formulations.

3.7. *Fourier transform infrared spectroscopy (FTIR)*

According to the FTIR spectra (Fig. 4), existence of peak at 1733 cm^{-1} indicates the presence of polymer in nanoparticles due to its steric carbonyl group, also existence peaks at 3443 cm^{-1} (stretch N–H secondary amine group) and 1475–1635 cm^{-1} (aromatic ring) in the nanoparticles confirm loaded drug on nanoparticle. IR spectra were observed which is probably due to the shift of the stretch ester carbonyl stretching peak of the hydroxyl and amine functional groups at 3443 cm^{-1} and 3494 cm^{-1} in Lidocaine hydrochloride, which could be related to the inhibition of the intramolecular hydrogen bindings, causing the enforcement of –NH and –OH bonds. Moreover, the stretching peak at 1733 cm^{-1} is related to the shifted carbonyl group peak in Eudragit RS-100 which shifted to the higher wavelength presenting the strengthening of this bond because of increased polarity. This is most probably because of the attraction of the polymer steric oxygen by the hydroxyl groups of Lidocaine hydrochloride. The evaluation of the IR spectra of the polymer, drug and nanoparticles indicated physical interactions between the drug and the polymer which lowered the intensity of the above peaks. These hydrogen bindings interactions could stabilize both the drug and the polymer, as discussed in DSC analysis, already. The hydrogen bindings between the functional groups of the drug and polymer were also reported by Adibkia *et al.*[23]

Spectrum of Lidocaine showed the presence of the following characteristic peaks: N–H stretching at 3443 cm^{-1}, C=O stretching at 1635 cm^{-1}, O–H stretching at 3494 cm^{-1}. In physical mixtures (1:1 and 1:2), the Lidocaine characteristic peak can still be detected, which indicates the presence of uncomplexed Lidocaine in physical mixtures.

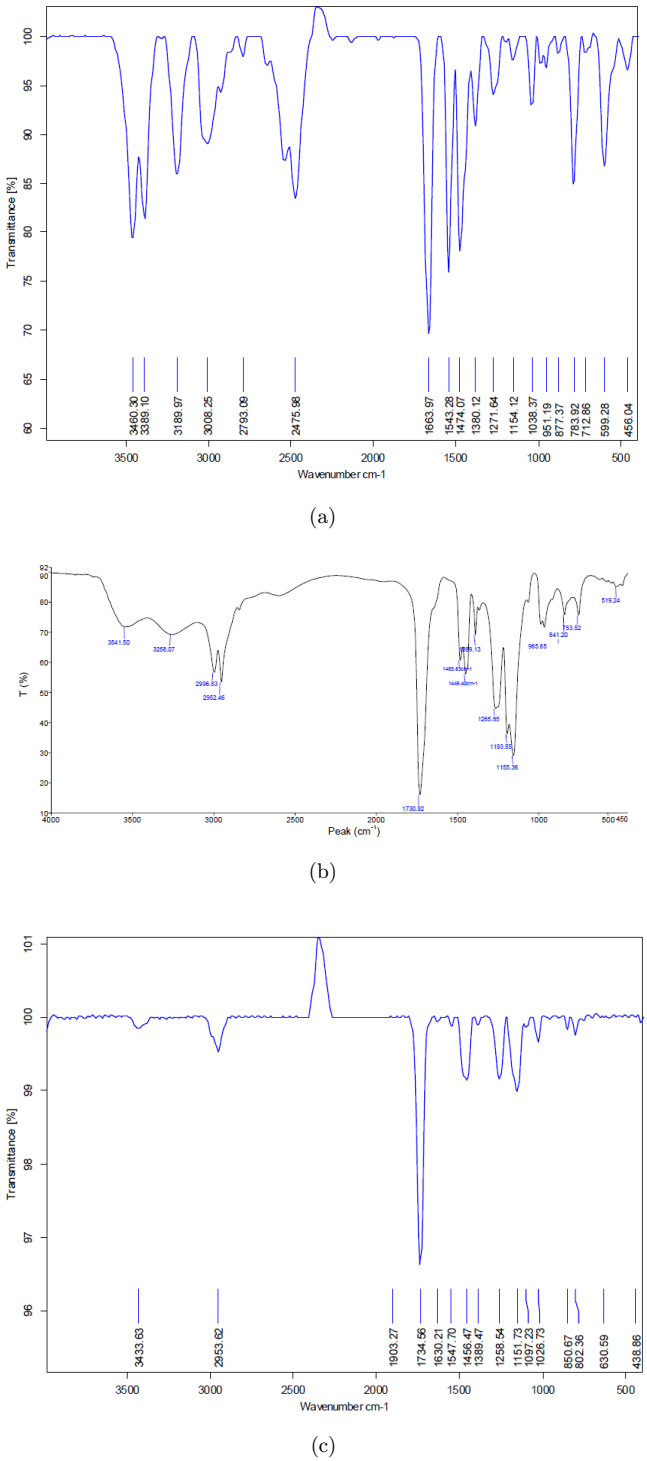

Fig. 4. FTIR spectrum of (a) Lidocaine hydrochloride, (b) Eudragit RS-100 and (c) F_b formulation.

The complete disappearance of the Lidocaine characteristic peak at 3443 cm^{-1}, 3494 cm^{-1} and 1635 cm^{-1} in inclusion complexes (1:1 and 1:2) can be attributed to the inclusion of functional groups of Lidocaine into the nanoparticles.

3.8. *Dissolution test in phosphate buffer*

Three formulations showed an initial burst drug release of nearly 20% after 30 min (Fig. 5). Burst release commonly occurs in release profile of almost all nanospheres made by solvent evaporation technique. It is supposed to be due to the erosion of the particles surface and releasing of the drug situated near the surface of the nanoparticles and adsorbed by the electrostatic attraction.[24]

The erosion of the nanoparticles wall, dissolution and diffusion of the drug into the dissolution medium seems to be the main mechanism for the sustained drug release from nanoparticles following the burst release. The rate of the drug dissolution and diffusion from the polymer determines the release pattern. The more drug released, the more formation of pores facilitates the faster drug release. Burst releasing could improve the drug penetration, while sustained releasing delivers the drug to the absorption site during a long period of time.[23]

F_c did not release the drug completely after 24 h and only about 90% had been released at the end of the test, while F_a released the close all drug after 24 h. Mady also reported the incomplete Ibuprofen release from the Eudragit RS-100 microspheres. Results of various trials show that the incomplete drug release is frequent when applying solvent evaporation technique. It has been discussed that this could be the result of drug-polymer interactions, or of the retarding property of the polymer.[24,25] Spenlehaur *et al.* proposed that the incipient drug release is due to great drug solubility in the polymer matrix or the penetration of the sink medium into the microspheres.[26]

The hydrophilic nature of Eudragit RS-100 facilitates the solubility of Lidocaine hydrochloride in the polymer matrix. The amount of the polymer–NH_3 groups in F_c that physically interacts with the drug–OH groups is more than F_a. These hydrogen bonding interactions, as explained by DSC and FTIR analysis, could probably result in less swelling of Eudragit RS-100 after the absorption of the dissolution medium and reduce the drug diffusion out from the gel layer formed by water absorption. The relation between the swelling properties of the excipients and drug release profile was shown in different studies.[27–29]

Moreover, the higher amount of the polymer in F_c makes the nanoparticle wall more coherent which makes it difficult for the dissolution liquid to penetrate into the particles and dissolve the drug.[18] The polymer structural network in F_a is looser compared to F_c. There didn't exist any significant difference between the percentage of the drug release from F_a, F_b and F_c at the end of 24 h (p value > 0.05).

3.8.1. *Dissolution kinetic*

High correlation was observed for Weibull ($R^2 = 0.942$), first order ($R^2 = 0.975$) and Logarithmic-probability ($R^2 = 0.995$) models for formulations. Corresponding Fick's law, the initial fast drug release is controlled by the nanoparticles wall erosion and the drug diffusion rate. After the occurrence of sink and stable condition, the constant diffusion rate was observed. Because, after the saturation of the dissolution medium, the drug concentration has minor effect on the release rate. The n value of equation was 1.417 for F_b indicating that the mechanism of the drug release was mainly controlled by the polymer erosion and in a less extent diffusion.

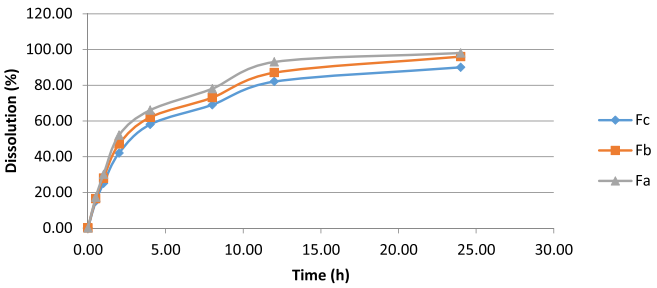

Fig. 5. The release profile of F_a, F_b and F_c in phosphate buffer (pH = 7.4).

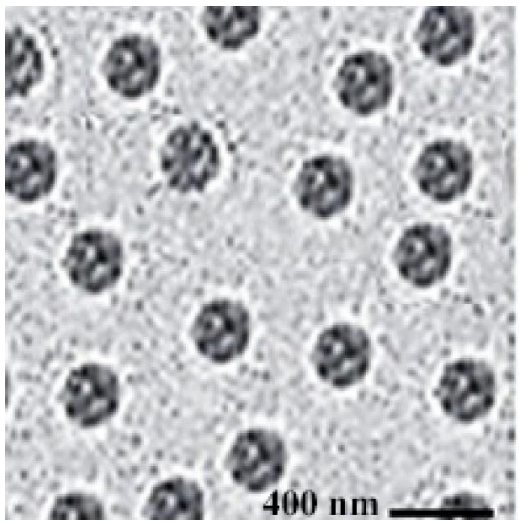

Fig. 6. TEM image of F_b formulation.

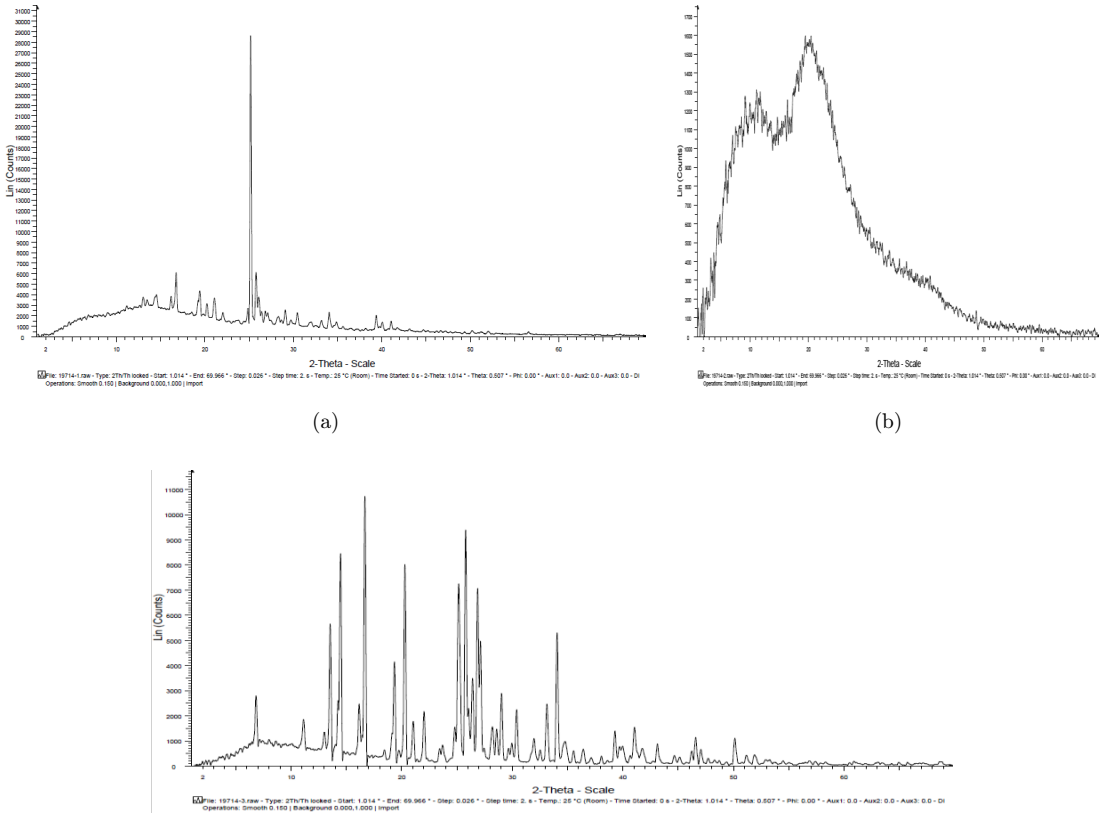

Fig. 7. XRD patterns of: (a) Lidocaine HCl, (b) Eudragit RS-100 and (c) Fb formulation.

4. Discussion

Use of Eudragit RS-100 and poly vinyl alcohol for the preparation of nanoparticles has been reported in the writing. It was thought usable to use a certain amount of them to assess the effect of composition on loading efficiency. It was found that increasing the ratio of polymer to drug leading to increases the loading efficiency. Moreover, under the experimental conditions, the total amount of drug and polymer and the speed of stirring play an essential role considering loading efficiency of nanoparticles. Increasing the Polymer/drug ratio increased the loading efficiency.

It has been reported that decreasing the particle size leads to an occlusive effect on the skin layer which leads to long operational time of the drug. This work manifested that increase polymer to drug ratio leading to increases the particle size. One probable cause for this could be the increase in viscosity of operating environment phase which leads to increase in the particle size of nanoparticles.

TEM photomicrographs of formulations manifest the almost spherical shape of nanoparticles with some nonuniformities at the edges of particulate carriers Fig. 6. The nonuniformities could be owing the method of preparation. The probe sonicator exertion high frequency waves might cause nonuniformities on the particle surface analogized to the solvent diffusion and solvent injection methods which are reported to lead smoother and spherical surface. The amount of polymer affects the permeability, leakage rates and overall stability of the nanoparticles. DSC studies give a vision of the phase transition in nanoparticles that are liable for the change in physical state of the system.

The height of the endotherm in the thermal scan of nanoparticles is less than that of the physical mixture which was formulated with the same component and ratio as that of nanoparticles. This proposes reduction of crystallinity of the Lidocaine after its incorporation into nanoparticles. The nanoparticles showed a mild beginning of dissolution, which gave a reason for the good solubilization capacity of the polymer which remained the drug in it and led to a primary slow release. The nanoparticles, which lack polymer matrix miscarried to retard the permeation of Lidocaine and complete penetration of Lidocaine, were observed at the end

of 12 h. It has been reported that as the polymer content of the nanoparticles dispersion increases, the formulation converts into gel with particulate aggregation and caters increase in skin permeation. Also, though surfactants help in maintaining the material polymorphism, they may also function as permeation enhancers.[30]

Our XRD patterns show an acceptable molecular arrangement for F_b formulation which give us good details about phase identification and crystallinity of our formulation Fig. 7.

The *in vivo* efficacy of the Lidocaine nanoparticulate systems was assessed on guinea pigs using the pinprick test. The traditional marketed gel formulation had a fast beginning of action and the skin was totally anesthetized. This showed that the ionized form of Lidocaine permeated much more rapidly than the free base but was rapidly absorbed and wears off by the cutaneous capillaries.

The nanoparticles formulation had a moderate beginning of action and the total time of profound local anesthesia lasted for 2–2.5 h, while the total time of anesthesia was up to 6–7 h. The formulations on the skin surface would release the drug leisurely which together with the free drug in the hydrogel matrix would permeate the stratum corneum. Furthermore, the drug would penetrate the upper part of stratum corneum and get mixed with the skin lipids thereby acting as a reservoir from which the drug was released slowly.

Acknowledgments

The authors disclosed receipt of financial support for the research, from Vice-Chancellor for Research Affairs of Ahvaz Jundishapur University of Medical Sciences (Grant No. N-114).

References

1. A. Scriabine, Discovery and development of major drugs currently in use, in *Pharmaceutical Innovation: Revolutionizing Human Health*, Vol. 148, (1999), p. 270.
2. C. Wasson *et al.*, Pharmacology of local anesthetic drugs, in *Absolute Obstetric Anesthesia Review* (Springer, 2019), pp. 27–29.
3. S. Yu *et al.*, *Int. J. Clin. Exp. Med.* **12**, 13203 (2019).
4. G. L. Liu, W. C. Bian, P. Zhao, L. H. Sun, *Curr. Drug Metab.* **20**(6), 533 (2019).
5. F. Arriagada and J. Morales, *Curr. Pharm. Des.* **25**, 455 (2019).
6. M. Franz-Montan *et al.*, *J. Liposome Res.* **25**, 11 (2015).
7. R. V. Gundloori, A. Singam and N. Killi, Nanobased intravenous and transdermal drug delivery systems, in *Applications of Targeted Nano Drugs and Delivery Systems* (Elsevier, 2019), pp. 551–594.
8. V. P. Chavda and D. Shah, *Trends Drug Deliv.* **3**, 25 (2019).
9. S. R. Mudshinge *et al.*, *Saudi Pharm. J.* **19**, 129 (2011).
10. K. N. Clayton *et al.*, *Biomicrofluidics* **10**, 054107 (2016).
11. T. Çomoğlu, N. Gönül and T. Baykara, *Il Farmaco* **58**, 101 (2003).
12. M. Bogataj *et al.*, *J. Microencapsul.* **8**, 401 (1991).
13. MRSEC. X-ray Diffraction Shared Experimental Facility. The MIT Materials Research Science and Engineering Center (MRSEC). Available from: http://prism.mit.edu/xray/. Accessed 29 November 2019.
14. J. D. Clogston and A. K. Patri, Zeta potential measurement, in *Characterization of Nanoparticles Intended for Drug Delivery* (Springer, 2011), pp. 63–70.
15. European Medicines Agency. Stability Testing of New Drug Substances and Products. 2003. Available from: https://www.ema.europa.eu/en/documents/scientific-guideline/ich-q-1-r2-stability-testing-new-drug-substances-products-step-5_en.pdf. Accessed 31 October 2019.
16. M. Barzegar-Jalali and S. Dastmalchi, *Drug Dev. Ind. Pharm.* **33**, 63 (2007).
17. Y. Li *et al.*, *Int. J. Pharm.* **490**, 324 (2015).
18. B. Nath, L. K. Nath and P. Kumar, *Acta Pol. Pharm.* **68**, 409 (2011).
19. K. Adibkia *et al.*, *J. Ocul. Pharmacol. Ther.* **23**, 421 (2007).
20. M. Danaei *et al.*, *Pharmaceutics* **10**, 57 (2018).
21. W. Zhang *et al.*, *Int. J. Nanomed.* **9**, 4305 (2014).
22. N. Tiong and A. A. Elkordy, *Eur. J. Pharm. Biopharm.* **73**, 373 (2009).
23. K. Adibkia *et al.*, *Colloids Surf. B, Biointerfaces* **83**, 155 (2011).
24. O. Mady, *MOJ Bioequiv. Bioavailab.* **4**, 193 (2017).
25. Y. D. Reddy, D. Dhachinamoorthi and K. C. Sekhar, *J. Chem. Pharm. Res.* **7**, 19 (2015).
26. G. Spenlehauer, M. Veillard and J. P. Benoit, *J. Pharm. Sci.* **75**, 750 (1986).
27. J. Armand *et al.*, *Int. J. Pharm.* **40**, 33 (1987).
28. D. Babay, A. Hoffman and S. Benita, *Biomaterials* **9**, 482 (1988).
29. D. Perumal *et al.*, *J. Microencapsul.* **16**, 475 (1999).
30. R. H. Müller, K. Maèder and S. Gohla, *Eur. J. Pharm. Biopharm.* **50**, 161 (2000).